14th European Signal Processing Conference (EUSIPCO 2006), Florence, Italy, September 4-8, 2006, copyright by EURASIP

SEGMENTATION OF ECHOCARDIOGRAPHIC IMAGES BASED ON STATISTICAL MODELLING OF THE RADIO-FREQUENCY SIGNAL

Olivier Bernard[1], Jan D'hooge[2], and Denis Friboulet[1]

[1]CREATIS, UMR CNRS 5515, U 630 INSERM, INSA
Blaise Pascal, 69621, Villeurbanne, France
phone: + (33) (0)4 72 43 64 07, fax: + (33) (0)4 72 43 85 26, email: olivier.bernard@creatis.insa-lyon.fr
[2]Cardiac Imaging Research (CIR), Dept. Of Cardiology
Herestraat 49, B-3000, Leuven, Belgium
email: jan.dhooge@uz.kuleuven.ac.be

ABSTRACT

This work presents an algorithm for segmentation of ultrasound images based on the statistics of the radio-frequency (RF) signal. We first show that the Generalized Gaussian distribution can reliably model both fully (blood pool) and partially (tissue area) developed speckle in echocardiographic RF images. We then show that this probability density function (pdf) may be used in a maximum likelihood framework for tissue segmentation. Results are presented on both simulations and ultrasound cardiac images of clinical interest.

1. INTRODUCTION

Segmentation of medical ultrasound is generally based on the analysis of B-scan images that are constructed from the envelope of the echo signal. In this context, different methods such as Markov random field [1], snakes and active contours [2], active shape and appearance models [3] or level set techniques [4] [5] have been proposed to deal with segmentation of echocardiographic images. In this work we propose to deal with ultrasound tissue segmentation using a statistical framework. Statistics of the ultrasound echo envelope have been extensively studied for both segmentation [1], [4] and tissue characterization [6], [7], [8] purposes. The most commonly used statistical model for the envelope signal is the conventional Rayleigh distribution which relies on the assumption of a large number of scatterers per resolution cell. In echocardiography, this model is particularly well suited to characterize reflections from blood but fails to model more complex structures such as myocardial tissue. *K* distributions have therefore been proposed to model different kinds of tissue in ultrasound envelope imaging [9], [10], [11]. This distribution has also the advantage to model both fully and partially developed speckle.

With the introduction of digital ultrasound devices, the radio-frequency signal has become more readily available. The interest of such signal resides in the fact that it potentially contains more information than the envelope echo. While it is well-known that the assumption of a large number of scatterers per range cell yields Gaussian statistics for the RF signal [7], very few studies have been devoted to the statistics of the RF signal in the case of partially developed speckle. Thus, from *K* distribution framework, we derived in [12] expressions for such statistics and applied them to echocardiographic RF data. In [13] we also demonstrated that this model can faithfully be approximated by the Generalized Gaussian (G.G.) distribution. This distribution has the advantage to yield simple expressions and robust parameters estimation for both fully and partially developed speckle. In section 2, a summary of the statistical modelling of the RF signal is presented. In section 3 we propose to exploit the Generalized Gaussian distribution in a maximum likelihood framework in order to perform tissue segmentation. Finally, the ability of the proposed method to segment echocardiographic images from RF signal is evaluated in section 4 from both simulations and data acquired in vivo.

2. STATISTICAL MODEL

The *K* distribution has been initially designed for the envelope signal [8]. The interest of such distribution in echocardiographic images relies on its ability to model both fully speckle (blood pool) and partially developed speckle (tissue area) situations. We briefly recall in this section the assumptions attached to the *K* distribution and give the corresponding pdf for the RF signal (detailed derivation can be found in [12]). The backscattered ultrasonic signal results from the individual energy contributions of each scatterer embedded in the resolution cell. This situation can mathematically be described as a random walk in the complex plane [9]. From this random flight model, the analytic signal can be expressed as a random process depending on the number of scatterers present inside the resolution cell, their relative position and contribution. Thus, a joint density function of the envelope and phase can be obtained by expressing both statistical properties of the phase and amplitude of each scatterer. This results in a *K* distribution when the scatterers phase is assumed to be uniformly distributed [10] and when their amplitude is modelled as a *K* distribution itself [11].

2.1 Physical Model: K_{RF} distribution

The RF signal corresponds to the real part of the analytic signal. The pdf of the RF signal thus corresponds to the marginal distribution obtained by integrating the pdf corresponding to the analytic signal with respect to its imaginary part, which yields the following expression (see [12] for details):

$$f_X^{rf}(x) = \frac{b}{\sqrt{\pi}\Gamma(\nu)}\left(\frac{b|x|}{2}\right)^{\nu-0.5} K_{\nu-0.5}(b|x|) \qquad (2)$$

where Γ is the Gamma function and $K_{\nu-0.5}$ is the modified Bessel function of the second kind of order $\nu-0.5$.
This expression is completely specified by its two parameters ν & b, such that ν controls the shape and b the scale of the pdf.
The corresponding distribution is called K_{RF} distribution in the following. This pdf may thus provide the basis for segmentation of echocardiographic images in the case of partially developed speckle, using for instance statistics-based active contours [5]. K_{RF} distribution however has the following drawbacks:

- Numerical simulation show that estimation bias grows rapidly as parameter ν increases, yielding unreliable estimates in blood regions (i.e. $\nu >> 1$);
- Equation (2) implies repeated evaluation of a Bessel function, increasing the computational cost of the algorithm.

2.2 Modelling RF signal statistics using Generalized Gaussian

From the observation that fully speckle situations correspond to a Gaussian pdf and non-fully speckle situations yields Laplacian-like distribution, we showed in [13] that the Generalized Gaussian distribution (G.G.) is a good candidate for approximating (2). G.G. has the following expression:

$$g_X^{rf} = \frac{\beta}{2.\alpha.\Gamma(1/\beta)}\exp\left(-\left(\frac{|x|}{\alpha}\right)^{\beta}\right) \qquad (3)$$

β &α are the two parameters of the distribution where β controls the shape and α the scale of the pdf. The G.G. pdf corresponds to a Gaussian distribution when $\beta = 2$ and to a Laplace distribution when $\beta = 1$.
This distribution has the advantage to have a simple expression with robust parameters estimation. In Figure 1, an example of the fit obtained for a parasternal long axis view in the myocardial tissue is given. This example illustrates qualitatively how the K_{RF} and Generalized Gaussian distributions better fits the data than the reference Gaussian. The ability of the proposed distributions to model the RF data has also been evaluated quantitavely through the root mean square error (RMSE). The results shown in Figure 1 yields a lower RMSE for the K_{RF} (57) and the Generalized Gaussian (67) than the Gaussian (311). K_{RF} and Generalized Gaussian distributions are so closed that it is difficult to separate them from the graph.

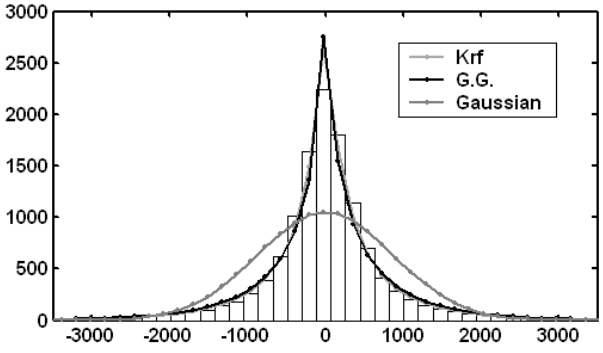

Figure 1 - Fits of the proposed distributions to the RF data from a parasternal long axis view in the myocardial tissue. The resulting RMSE associated to the K_{RF}, Generalized Gaussian and the Gaussian is respectively 57, 67 and 311.

The ability of the G.G. to model cardiac RF data observed on the example given in Figure 1 has been validated on a set of ultrasound cardiac images including every orientations used in clinical practice [13].

3. SEGMENTATION METHOD

We showed that the G.G. distribution is an interesting model for both tissue and blood characterisation. Thus, we propose in this part to exploit this distribution for ultrasound tissue segmentation.

3.1 Energy Functional

The framework we use for segmentation is based on the approach described by Zhu & Yuille in [14]. In order to evaluate the performance of the chosen distribution, we use the statistics of the image as the only information source, without any additional terms (as for example the a priori knowledge about the shape of the object to be detected). One of the common approaches in this context is the use of the Maximum Likelihood (ML) method [15]. Let us consider an ultrasound image as a random field where the values of the signal at each pixel are assumed to be independent. Now consider an active contour Γ partitioning the image into two domains Ω_{in} and Ω_{out}. The ML method consists in finding the minimum of the following energy criterion:

$$l(I,\Gamma) = \iint_{\Omega_{in}} -\log p_{in}(I/\alpha_{in})\, dxdy + \iint_{\Omega_{out}} -\log p_{out}(I/\alpha_{out})\, dxdy \qquad (4)$$

where p_{in} and p_{out} are some a priori distributions with respectively parameters α_{in} and α_{out}. Using gradient descent method, a local minimum of (4) can be obtained using the following evolution equation:

$$\frac{\partial\Gamma}{\partial\tau} = \left(-\log p_{in}(I_c/\alpha_{in}) + \log p_{out}(I_c/\alpha_{out})\right).\vec{N} \qquad (5)$$

where N is the inward normal to the contour, τ is the temporal evolution parameter and I_c is a pixel lying on Γ.

The evolution term given in (5) allows to reliably segment two regions, provided the corresponding statistics have distinct, well-separated means.
In the case of echocardiographic RF data, the statistics of the two regions to be segmented (i.e. blood pool and myocardium) have equal zero means. As shown by Zhu & Yuille [14], this specificity can be easily accounted for by using the joint probability of the intensities included in a window centred on each pixel. This is equivalent to replace $p(I_{(x,y)}/\alpha)$ in equation (5) by the following joint probability:

$$\prod_{(u,v)\in W(x,y)} P(I_{(u,v)}/\alpha) \qquad (6)$$

where $W_{(x,y)}$ represents a circular window centred at pixel $I_{(x,y)}$ of size m.

3.2 Parameters estimation

The evolution given in (5) implies estimation of the parameters of the a priori distributions p_{in} and p_{out} at each iteration. The estimation of the G.G. parameters has been thoroughly investigated [16] [17]. Basically two different ways to estimate the scale and shape parameters from available sample data exist. Maximum likelihood-based method gives the optimal estimation parameters given observed samples. For the G.G. case, this method leads to a closed form solution whose expressions are complex and time consuming. To overcome these difficulties, a method based on the first and second moment of the G.G. distribution has been proposed [17]. The consistency of these two estimators has been evaluated in terms of bias and variance. Data distributed according to the pdf given in equation (3) were generated using the Cumulative Distribution Function (CDF) method [18]. The number of data samples (N) was chosen to be 1024. This procedure was repeated 1000 times and the corresponding bias and variance are presented in table 1.

	ML method		Moment method	
β	Bias	Variance	Bias	Variance
0.4	0.0267	0.00037	0.0815	0.00047
0.8	0.0166	0.0021	0.0319	0.0020
1.2	0.0106	0.0055	0.0115	0.0056
1.6	0.0168	0.0115	0.0168	0.0115
2.0	0.0203	0.0215	0.0240	0.0248

Table 1 - Comparison of the estimated Bias and Sample Variance of β for ML and moment methods for N=1024

Table 1 shows that the results of the moment-based method converge to the results of the ML method for values of β ranging between 1.2 and 2.0. For β lower than 1, the bias estimated from the moment method increases dramatically in comparison with the bias obtained from the ML method. From these results, we decided to use the ML method to ensure good parameters estimation during the evolution process. The ML expressions used to estimate β & α from a sample {x1,x2,…,xN} of size N are the following:

$$1+\frac{\Psi(1/\beta)}{\beta}-\frac{\sum_{i=1}^{N}\log|x_i|.|x_i|^{\beta}}{\sum_{i=1}^{N}|x_i|^{\beta}}+\frac{\log\left(\frac{\beta}{N}\sum_{i=1}^{N}|x_i|^{\beta}\right)}{\beta}=0 \qquad (7)$$

and

$$\alpha=\left(\frac{\beta}{N}\sum_{i=1}^{N}|x_i|^{\beta}\right)^{\frac{1}{\beta}} \qquad (8)$$

where Ψ is the digamma function.

3.3 Implementation of the evolution using level sets

The evolution of the active contour Γ has been implemented using a Level Set approach. This technique has the advantage to be topology free which makes the algorithm less sensitive to the initialisation. Moreover, we implemented our algorithm using a sparse-field technique proposed by Whitaker in [19]. This technique has the advantage to significantly decrease the computing time by working on a narrow band.

4. RESULTS

4.1 Simulation results

The proposed method has been tested on a simulated image given in figure 2. This image consists of three regions generated using G.G. distributions with different parameters. These parameters have been chosen from real data corresponding to a parasternal long axis orientation. Thus region 1 has parameters values corresponding to blood pool and region 2 and 3 have parameters values corresponding to tissue area. Table 2 summarizes parameters values associated with each region.

Region	β	α	Simulated cardiac area
1	2.0	85	Blood
2	0.58	180	Interventricular Septum
3	1.45	555	Left Ventricle infero-lateral wall

Table 2 - G.G. parameters values describing the different regions of the simulated image

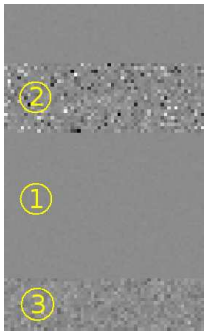

Figure 2 - Simulated image from G.G. distributions.

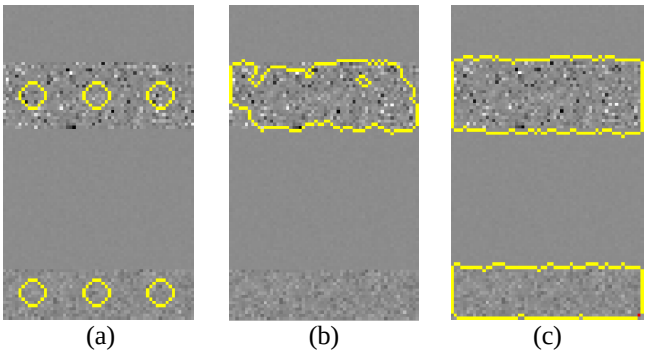

Figure 3 - Segmentation of the simulated image. (a) Initialisation. (b) Segmentation result obtained when a Gaussian pdf is used for the evolution. (c) Segmentation result obtained when a Generalized Gaussian pdf is used for the evolution.

Figure 3 shows the initialisation of the active contour on the simulation image and shows a comparison of the results obtained when a standard Gaussian or the proposed Generalized Gaussian is used as the a priori pdf in the evolution term given in (5).
It is seen from figure 3(b) that the active contour properly segments region 1 but fails to segment region 3 (bottom of the image) when the evolution is driven through a Gaussian pdf. This is easily explained by the fact that region 3 is statistically close to adjacent region 1: the shape parameter β of the G.G. used to generate region 1 is set to 2 (i.e. Gaussian statistics corresponding to blood) and region 3 (left ventricle infero-lateral wall) was generated using β=1.45. These two regions can therefore not be separated using simple Gaussian pdf in the evolution term.
On the opposite, figure 3(c) shows that the flexibility of the G.G. used in the evolution allows for proper segmentation of regions 2 and 3 from region 1.

4.2 Results from in vivo data

The ability of the proposed method to segment echocardiographic images from RF signal using Generalized Gaussian was tested on ultrasound cardiac images acquired in vivo. Data were acquired using Toshiba Powervision 6000 (Toshiba Medical Systems Europe, Zoetermeer, the Netherlands) equipped with an RF interface for research purposes and a 3.75 MHz-probe. The RF sample frequency varied between 25 and 32 MHz according to the acquisition mode.
Figure 4 shows the result obtained for a parasternal long axis view. Figure 4(a) shows the initialisation of the active contour and figure 4(b) and 4(c) show the results obtained when respectively a standard Gaussian and a Generalized Gaussian distribution are used as the a priori pdfs. This configuration is close to the simulation experiment previously discussed: the myocardium is seen as two disconnected regions (interventricular septum and infero-lateral wall) with dissimilar statistical properties. Result shows in figure 4(b) is in agreement with the ones obtained in the simulation part: the Gaussian distribution is not

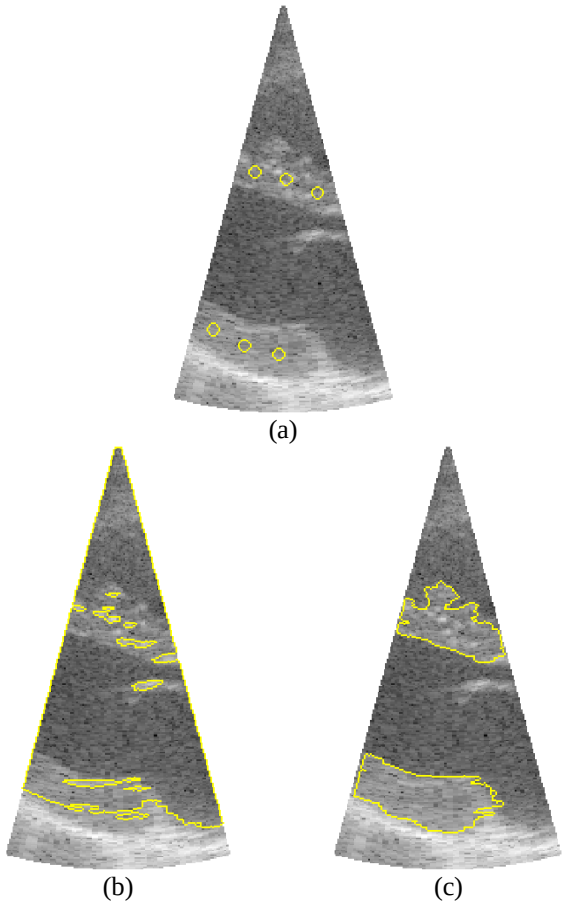

Figure 4 - Segmentation of an echocardiographic image acquired in vivo for a Parasternal long axis orientation. (a) Initialisation. (b) Segmentation result obtained when a Gaussian pdf is used for the evolution. (c) Segmentation result obtained when a Generalized Gaussian pdf is used for the evolution.

appropriate to characterize myocardium region in a maximum likelihood approach. On the opposite, figure 4(c) indicates that the proposed approach yields proper segmentation of the myocardium, owing again to the G.G. pdf modelling of the RF signal. As previously mentioned, it is to be noted that the algorithm purposely uses the statistics of the RF image as the only information source, without any additional terms (such as the conventional curvature term), which explains the fact that the obtained contours are not smooth. Such terms could obviously be added to the evolution term (5) to enforce smoothness of the contour.
Figure 5 shows the results obtained for an apical 4 chamber view. Figure 5(a) shows the initialisation of the active contour and figure 5(b) and 5(c) show the results obtained when respectively a standard Gaussian and a Generalized Gaussian distribution are used as the a priori pdfs. Here again the active contour driven by the G.G. pdf provides a better segmentation of the septum.

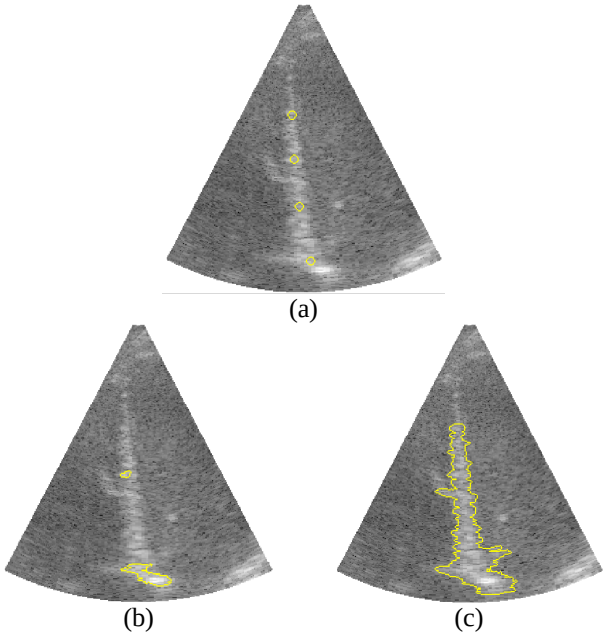

Figure 5 - Segmentation of an echocardiographic image acquired in vivo for an Apical 4 chamber orientation. (a) Initialisation. (b) Segmentation result obtained when a Gaussian pdf is used for the evolution. (c) Segmentation result obtained when a Generalized Gaussian pdf is used for the evolution.

5. CONCLUSION

We have presented in this paper a maximum-likelihood approach for segmentation of echocardiographic images based on modelling the statistics of the radio-frequency (RF) signal through a Generalized Gaussian distribution.

The interest of this distribution relies on the fact that it provides a reliable model for both fully and partially developed speckle, which occurs respectively in blood and myocardial regions of the cardiac images.

Simulation results indicate that this versatility allows to segment regions which would be otherwise statistically too close to be properly separated by using a conventional Gaussian modelling. Results obtained from in vivo echocardiographic data acquired in parasternal long axis and apical 4 chamber views show that the proposed approach yields proper segmentation of the myocardial tissue.

Future work includes enhancing the proposed segmentation approach by constraining the evolution of the active contour through shape and motion a priori.

REFERENCES

[1] L. Herlin, D. Bereziat, G. Giraudon, C. Nguyen and C. Graffigne, "Segmentation of echocardiographic images with Markov fields," *Proc. Eur. Conf. Comput.* Vision, pp. 201-206, 1994.

[2] D. Linker and V. Chalana, "Active Contour Model for Cardiac Boundary Detection on Echocardiographic Sequences," *IEEE Trans. Med. Imag.*, vol. 15, pp. 290-298, 1996.

[3] S. Zhou, D. Comaniciu, and A. Krishnan, "Coupled-Contour Tracking through Non-orthogonal Projections and Fusion for Echocardiography," *European Conference on Computer Vision.*, vol. 1, pp. 336-349, 2004.

[4] A. Sarti, C. Corsi, E. Mazzini, and C. Lamberti, "Maximum Likelihood Segmentation of Ultrasound Images with Rayleigh Distribution," *Pattern Recognition Lett.*, vol.24, pp. 779-790, 2003.

[5] I. Dydenko, F. Jamal , O. Bernard, J. D'hooge, I.E. Magnin, and D. Friboulet, “A level set framework with a shape and motion prior for segmentation and region tracking in echocardiography,” *Medical Image Analysis*, 2005, in press.

[6] P.M. Shankar et. al., "Classification of breast masses in ultrasonic B scans using Nakagami and K distributions," *Phys. Med. Biol.* 48 pp. 2229-2240, 2003.

[7] R. F. Wagner, M. F. Insana and D. G. Brown, "Statistical properties of radio-frequency and envelope-detected signals with applications to medical ultrasound, "*J. Opt. Soc. Am. A*, vol. 4, pp. 910–22, 1987.

[8] P.M. Shankar, "A model for ultrasonic scattering from tissues based on the K distribution," *Phys. Med. Biol.* 40 pp. 1633-1649, 1995.

[9] K. Pearson, "The problem of the random walk," *Nature*, vol. 72, pp. 294, 342, 1905.

[10] J. W. Goodman, *Statistical Optics*, New York: Wiley, pp. 44-55, 533-3817, 1985.

[11] E. Jakeman and P.N. Pusey, "A Model for Non-Rayleigh Sea Echo," *IEEE Trans. Antennas Propagat.*, Vol 24, N°6, 1976.

[12] O. Bernard, J. D’hooge, and D. Friboulet, "Statistics of the radio-frequency signal based on k distribution with application to echocardiographic images," *IEEE Trans. Ultrason., Ferroelect., Freq. Contr.*, 2005, submitted

[13] O. Bernard, J. D’hooge, and D. Friboulet, "Statistical modelling of the radio-frequency signal in echocardiographic images based on Generalized Gaussian distribution," in *Proc. ISBI*, 2006, accepted.

[14] S. Zhu, and A. Yuille, "Region competition: unifying snakes, region growing, and Bayes/MDL for multiband image segmentation," *IEEE Trans. Pattern Anal.Machine Intell.*, Vol 18, pp. 884-900, 1996.

[15] A. Azzalini, *Statistical Inference-Based on the Likelihood*. New York, Chapman and Hall, 1996.

[16] R. Krupinski, J. Purczynski, "Approximation fast estimator for the shape parameter of generalized Gaussian distribution," *Signal Processing*, 86, pp. 205-211, 2005.

[17] S.G. Mallat, "A theory of multiresolution signal decomposition: the wavelet representation," *IEEE Trans. Pattern Anal. Machine Intell.*, 11, pp. 674-693, 1989.

[18] A. Consortini and F. Rigal, "Fractional moments and their usefulness in atmospheric laser scintillation," *Pure and Applied Optics*, vol.7, pp. 1013-1032, 1998.

[19] R.T. Whitaker, "A leve-Set Approach to 3D Reconstruction from Range Data," *International Journal of Computer Vision* 29(3), 203-231, 1998.